

Variability of sea-salts in ice/firn cores from Fimbul Ice Shelf, Dronning Maud Land – DML, Antarctica

Carmen Paulina Vega,^{1,2,¶,§} Elisabeth Isaksson,¹ Elisabeth Schlosser,^{3,4} Dmitry Divine,¹ Tõnu Martma,⁵ Robert Mulvaney,⁶ Anja Eichler,⁷ and Margit Schwikowski-Gigar.⁷

5 ¹Norwegian Polar Institute, N-9296 Tromsø, Norway

²Department of Earth Sciences, Uppsala University, Villavägen 16, SE-75236, Uppsala, Sweden

³Institute of Atmospheric and Cryospheric Sciences, University of Innsbruck, Innsbruck, Austria

⁴Austrian Polar Research Institute, Vienna, Austria

⁵Department of Geology, Tallinn University of Technology, Tallinn, Estonia

10 ⁶British Antarctic Survey, Madingley Road, High Cross, Cambridge, Cambridgeshire CB3 0ET, United Kingdom

⁷Paul Scherrer Institute, 5232 Villigen PSI, Switzerland

Now at:

[¶]School of Physics, University of Costa Rica, San Pedro de Montes de Oca, 11501-2060 San Jose, Costa Rica

[§]Centre for Geophysical Research, University of Costa Rica, San Pedro de Montes de Oca, 11501-2060 San Jose, Costa Rica

15 *Correspondence to:* C. P. Vega (carmen.vegariquelme@ucr.ac.cr)

Abstract. Major ions were analysed in firn/ice cores located at Fimbul Ice Shelf (FIS), Dronning Maud Land – DML, Antarctica. FIS is the largest ice shelf in the Haakon VII Sea, with an extent of approximately 36 500 km². Three shallow firn cores (about 20 m deep) were retrieved in different ice-rises, Kupol Ciolkovskogo (KC), Kupol Moskovskij (KM), and Blåskimen Island (BI), while a 100 m long core (S100) was drilled near the FIS edge. These sites are distributed over the entire FIS area so that they provide a variety of elevation (50–400 m a.s.l.) and distance (3–42 km) to the sea. Sea-salt species (mainly Na⁺ and Cl⁻) generally dominate the precipitation chemistry in the study region. We associate a significant six-fold increase in median sea-salt concentrations, observed in the S100 core after the 1950s, to an enhanced exposure of the S100 site to primary sea-salt aerosol due to a shorter distance from the S100 site to the ice front, and to enhanced sea-salt aerosol production from blowing salty snow over sea ice, most likely related to the calving of Trolltunga occurred during the 1960s. This increase in sea-salt concentrations is synchronous with a shift in non-sea-salt sulfate (nssSO₄²⁻) toward negative values, suggesting a possible contribution of fractionated aerosol to the sea-salt load in the S100 core most likely originating from salty snow found on sea ice. In contrast, there is no evidence of a significant contribution of fractionated sea-salt to the ice-rises sites, where the signal would be most likely masked by the large inputs of biogenic sulfate estimated for these sites. In summary, these results suggest that the S100 core contains a sea-salt record dominated by the proximity of the site to the ocean, and processes of sea

ice formation in the neighbouring waters. In contrast, the ice-rises firm cores register a larger-scale signal of atmospheric flow conditions and a less efficient transport of sea-salt aerosols to these sites. These findings are a contribution to the understanding of the mechanisms behind sea-salt aerosol production, transport and deposition at coastal Antarctic sites, and the improvement of the current Antarctic sea ice reconstructions based on sea-salt chemical proxies obtained from ice cores.

5 **1 Introduction**

Antarctic ice and firn cores contain valuable information about the climate and atmospheric chemical composition of the past and provide evidence for the important role of Antarctica in the global climate system. Numerous ice and firn cores have been drilled in Antarctica during the past decades (Stenni et al., 2017). However, relatively few cores were drilled in coastal regions, which are more sensitive to changes in climate than the dry and cold interior of Antarctica. In fact, two recent review papers point out the lack of ice core data from low elevation coastal areas when discussing Antarctic climate variability (Stenni et al., 2017; Thomas et al., 2017). In an effort to understand the role of ice shelves in stabilizing the Antarctic ice sheet, particular focus has been laid on the investigation of ice-rises and ice-rumples as buttressing elements within the ice sheet - ice shelf complex (Paterson, 1994; Matsuoka et al., 2015). Furthermore, due to their radial ice flow regime, generally low ice velocities, and relatively high surface mass balance (SMB), ice-rises are potentially useful sites for ice core retrieval (Philippe et al., 2016; Vega et al., 2016). Firn and ice cores drilled at ice-rises allow obtaining high-resolution climate records to investigate sub-annual and long-term temporal changes in the loads of different chemical compounds found in the snow, providing information about their sources and transport, particularly of sea-salt ions, such as sodium (Na^+) and chloride (Cl^-), which are strongly modulated by sea ice extent and meteorological conditions. Recent modelling efforts to study the use of sea-salts as proxies for past sea ice extent have shown that, under present climate conditions and on interannual timescales, meteorological conditions rather than sea ice extent are the dominant factor modulating atmospheric sea-salt concentrations that are deposited at the interior and coastal sites in Antarctica (Levine et al., 2014). However, sea-salts have the potential as proxy for sea ice extent at glacial-interglacial scales when large changes in sea ice extent took place (Levine et al., 2014).

At most Antarctic sites, atmospheric sea-salt concentrations present maxima during austral winter (Wagenbach et al., 1998; Weller and Wagenbach, 2007; Jourdain et al., 2008; Udisti et al., 2012), with the exception of Dumont D'Urville where maxima occur during summer (Wagenbach et al., 1998). Similarly, sea-salt fluxes obtained from Antarctic ice cores also show winter maxima (Abram et al. 2013 and references therein). However, in some recent core records from coastal sites, no clear seasonality is observed, e.g. at Mill Island during the period 1934–2000 (Inoue et al., 2017). Abram et al. (2013) conclude that despite the seasonal signal registered in different Antarctic ice cores, sea-salt fluxes do not show a consistent relationship with sea ice extent on inter-annual timescales, and on the contrary, are highly dependent on atmospheric transport, and/or the presence of polynyas.

Hitherto, two main sources of increased winter sea-salt aerosols have been proposed: (i) increased storminess leading to an enhancement of sea-salt aerosols above the open ocean with possibly faster meridional transport (Petit et al., 1999; Fischer et

al. 2007), and (ii) a direct input of sea-salts associated to increases in sea ice, overcoming source (i), e.g. due to frost flowers (Rankin and Wolff, 2002; Rankin et al., 2004; Roscoe et al., 2011), brine (Rankin et al., 2000), and the contribution of snow transported over sea ice by wind (Yang et al., 2008, 2010; Huang and Jaeglé, 2017; Rhodes et al., 2017).

In the review by Abram et al. (2013), the authors suggest that the brine-frost flower system is a plausible source of sea-salt aerosols to coastal Antarctic sites. This hypothesis is supported by the experimental evidence that the original seawater $\text{SO}_4^{2-}/\text{Na}^+$ ratio cannot be used in the non-sea-salt sulfate (nssSO_4^{2-}) calculations, leading to negative nssSO_4^{2-} values both in winter aerosol and fresh snow sampled at coastal sites (Hall and Wolff, 1998; Wagenbach et al., 1998; Curran et al., 1998; Rankin and Wolff, 2002 and 2003), and also in ice cores from both inland (Wagenbach et al., 1994, Kreutz et al., 1998) and coastal sites (Inoue et al., 2017). These negative values indicate that a lower $\text{SO}_4^{2-}/\text{Na}^+$ ratio has to be used in nssSO_4^{2-} calculations, i.e., a depletion of SO_4^{2-} with respect to seawater composition occurred in wet and dry deposition.

During the process of sea ice formation, ions present in the water are not incorporated in the ice crystal matrix, but remain as highly concentrated brine in brine pockets or channels. The brine can be transported by capillary effects through brine channels to the newly formed ice surface, resulting in a thin layer of highly saline surface brine. This fractionated brine is unlikely to be a direct source of sea-salts because it usually quickly gets covered by snow, and no clear mechanism has been found to explain how this brine could become airborne (Abram et al., 2013). With further cooling of the ice, the volume of brine decreases and consequently, its salinity increases, leading to the precipitation of different saline compounds. This depends on temperature, e.g. sodium sulfate or mirabilite ($\text{Na}_2\text{SO}_4 \cdot 10 \text{H}_2\text{O}$) starts to precipitate at temperatures below -8°C , while sodium chloride (NaCl) at temperatures below -26°C . Consequently, the remaining brine is depleted in sodium and sulfate ions via precipitation of mirabilite at relatively mild polar temperatures. Frost flowers can form from this brine when meteorological conditions are adequate, i.e. at low intensity winds, which allows these delicate structures to grow without breaking apart, and on very thin ice where a strong temperature gradient is present between the ice surface and the overlying air (Rankin et al., 2000; Rankin and Wolff, 2002, and references therein). Thus, frost flowers formed at temperatures below -8°C will be depleted in sodium and sulfate relative to other ions present in seawater (Rankin et al., 2000; Rankin and Wolff, 2002), evidenced by negative nssSO_4^{2-} values measured in aerosols and snow (see section 2.3 for more details on the calculation of the nss -fractions).

For most of the last decade, frost flower formation, transport and deposition, has been considered the most plausible mechanism behind the fractionated aerosol detected at coastal areas. However, Yang et al. (2008 and 2010), and Huang and Jaeglé (2017) proposed an alternative mechanism: the origin of sea-salt aerosol could be due to the sublimation of blowing salty snow. This salty snow could be a result of frost flower formation, upward migration of brine within the snow (Massom et al., 2001), or by the input of sea-spray from the open ocean or nearby leads or polynyas (Dominé et al., 2004). Flooding of sea ice under the weight of accumulated snow can also induce increased salinity of snow (Massom et al., 2001). As the snow can be contaminated or wetted with fractionated brine or frost flowers, it could be expected that this salty snow also shows such fractionation. As pointed by Yang et al. (2008 and 2010), this salty snow can be transported by wind and if the air is not

saturated, the snow particles may lose water by sublimation and become sea-salt aerosols. These aerosols could then be transported and deposited either by dry or wet deposition, depending on local meteorology.

According to Abram et al. (2013), the idea proposed by Yang et al. (2008) is plausible for coastal sites, along with the frost flower mechanism. Consequently, snow present on new sea ice and frost flowers are features that, combined with wind transport, need to be taken into account when interpreting the sea-salt record of coastal ice and firn cores.

This study discusses sub-annual and long-term temporal changes in sea-salt and major ion concentration measured in three recently drilled firn cores from different ice-rises located at Fimbul Ice Shelf (FIS): Kupol Ciolkovskogo, Kupol Moskovskij, and Blåskimen Island, a 100 m long core drilled near the FIS edge (S100) (Figure 1). The main goals of the present study are to investigate possible mechanisms behind deposition, sub-annual, and spatial variability of sea-salts in this coastal region.

The results presented here contribute to bridging the data gap existent at coastal Antarctic sites, and to the improvement of current Antarctic sea ice reconstructions based on sea-salt chemical proxies.

2 Methods

2.1 Study area

With an extent of approximately 36 500 km², FIS is the largest ice shelf in the Haakon VII Sea (Figure 1). Fed by Jutulstraumen, the largest outlet glacier in DML, FIS is divided into a fast moving ice tongue, Trolltunga, directly feeding the central part of the ice stream, and slower surrounding parts. Several ice-rises (250–400 m a.s.l.; 10–42 km from the coast) are found at FIS, varying in size from 15 to 1200 km², and located approximately 200 km apart.

Early investigations in this area began during the International Geophysical Year (IGY) 1956/57 (Swithinbank, 1957; Lunde, 1961; Neethling, 1970) and continued during the last decades with focus on surface mass balance (SMB) variability in space and time (Melvold et al., 1998; Melvold, 1999; Rolstad et al., 2000; Isaksson and Melvold, 2002; Kaczmarska et al., 2004; Kaczmarska et al., 2006; Divine et al., 2009; Sinisalo et al., 2013; Schlosser et al., 2012, 2014; Langley et al., 2014; Vega et al., 2016). However, studies on spatial and temporal variability of chemical composition of snow and ice from this area are limited to water stable isotopes interpretations (Kaczmarska et al., 2004; Schlosser et al., 2012, 2014; Vega et al., 2016).

SMB obtained from the S100 core (Figure 1) retrieved at FIS shows a mean long-term accumulation rate of 0.3 m water equivalent per year (m w.e. yr⁻¹) for the period 1737–2000, with a significant negative trend in SMB for the period 1920–2000 (Kaczmarska et al., 2004). This negative trend in SMB has been reported in several shorter firn cores from the region (Isaksson and Melvold, 2002; Divine et al., 2009; Schlosser et al., 2014), including one record from the Kupol Ciolkovskogo ice-rise (Vega et al., 2016).

More detailed information on previous campaigns, glaciological and meteorological conditions at FIS and the core sites at the ice-rises, can be found in Vega et al. (2016) and Goel et al. (2017), and references therein, whereas an overview on Antarctic ice-rises is given in Matsuoka et al. (2015).

2.2 Sampling

Three shallow firn cores (about 20 m deep) were retrieved at different ice-rises (Kupol Ciolkovskogo (KC), Kupol Moskovskij (KM), and Blåskimen Island (BI), Figure 1, Table 1), located at FIS between January 2012 and January 2014 during field expeditions organized by the Norwegian Polar Institute (NPI). Location, elevation, and length of the different ice-rises cores are presented in Table 1. Each core was drilled from the bottom of a 2 m snow pit (not sampled for major ions). The firn density was determined as bulk density of each sub-core piece (average length of 45 cm). The samples were collected following clean protocols (Twickler and Whitlow, 1997), shipped frozen to NPI, and later to the Paul Scherrer Institute (PSI), Switzerland, for cutting and chemical analysis. Sample resolution varied between 4 and 8 cm depending on sample depth and density. Thickness of ice lenses, water stable isotope ratios and SMB for the three ice-rises are reported in Vega et al. (2016). Additionally, unpublished major ion concentrations measured in the 100 m deep S100 core drilled in austral summer 2000/2001 (Kaczmarek et al., 2004) were included in this study (Figure 1, Table 1). The S100 core was sampled at 5 cm resolution between top and 6 m deep, and then at 25 cm resolution between 6 m to 100 m deep.

2.3 Chemical analyses

Major ions (methanesulfonic acid (MSA), Cl^- , NO_3^- , SO_4^{2-} , Na^+ , K^+ , Mg^{2+} and Ca^{2+}) present in the three firn cores from the ice-rises were analysed at PSI using a Metrohm ProfIC 850 ion chromatograph combined with an 872 Extension Module and auto-sampler. The precision of the method was within 5 % and detection limits (D.L.) were below $0.02 \mu\text{mol L}^{-1}$ for each ion (Wendl et al., 2014). Ion concentrations (MSA, Cl^- , NO_3^- , SO_4^{2-} , Na^+ , K^+ , Mg^{2+} and Ca^{2+}) in the S100 core were measured at the British Antarctic Survey (BAS) using fast ion chromatography (Littot et al., 2002). The reproducibility of the measurements was 4–10 %.

Major ion concentrations were separated into sea-salt (ss) and non-sea-salt (nss) fractions calculated from the mean seawater composition using ssNa^+ as standard ion, as:

$$[\text{nssX}] = [\text{X}]_{\text{total}} - k_{\text{seawater}} \times [\text{ssNa}^+], \text{ and}$$

$$[\text{ssX}] = k_{\text{seawater}} \times [\text{ssNa}^+]$$

where

$$k_{\text{seawater}} = \frac{[\text{X}]_{\text{seawater}}}{[\text{Na}^+]_{\text{seawater}}}$$

with k_{seawater} values listed in Table S1 in the Supplementary material.

To calculate the ssNa^+ fraction, we used the following equations system, in which nssCa^{2+} was employed as reference ion to obtain the nssNa^+ associated to Earth's crustal material:

$$[\text{Na}^+]_{\text{total}} = [\text{ssNa}^+] + [\text{nssNa}^+]$$

$$[\text{Ca}^{2+}]_{\text{total}} = [\text{ssCa}^{2+}] + [\text{nssCa}^{2+}]$$

$$[\text{ssNa}^+]_{\text{total}} = [\text{Na}^+]_{\text{total}} - k_{\text{crustal}}[\text{nssCa}^{2+}]$$

$$[\text{nssCa}^{2+}]_{\text{total}} = [\text{Ca}^{2+}]_{\text{total}} - k_{\text{seawater}}[\text{ssNa}^+]$$

where $k_{\text{crustal}} = \frac{[\text{Na}^+]_{\text{crust}}}{[\text{Ca}^{2+}]_{\text{crust}}} = 1.40$ (using molar concentrations) (Lutgens and Tarbuck, 2012), and $k_{\text{seawater}} = \frac{[\text{Ca}^{2+}]_{\text{seawater}}}{[\text{Na}^+]_{\text{seawater}}} = 0.02$, (using

molar concentrations, Table S1) (Summerhayes and Thorpe, 1996).

- 5 Due to the low concentrations of NO_3^- in standard seawater (Summerhayes and Thorpe, 1996), NO_3^- was not separated into nss- and ss-fractions (i.e., NO_3^- was assumed to have a nss-origin only, as well as MSA).

In addition, water stable isotopes analyses of the KC, KM and BI cores are described in Vega et al. (2016); while analysis of the S100 core is described in (Kaczmarska et al., 2004).

2.4 Firm and ice core timescales

- 10 The timescales of the KM and BI cores were obtained based on annual layer counting of water stable isotope ratios ($\delta^{18}\text{O}$), and found to cover the periods between austral winter-1995(96) and summer-2014, respectively. The error in the dating was estimated as ± 1 year for both of these cores (Vega et al., 2016). Both KC and the S100 cores were dated using a combination of annual layer counting of $\delta^{18}\text{O}$ and identification of volcanic horizons, i.e. by using the SO_4^{2-} , dielectric profiling (DEP), and electrical conductivity measurements (ECM), with timescales covering the time period 1958–2012 (± 3 years) at KC (Vega et al., 2016), and 1737–2000 (± 3 years) at S100 (Kaczmarska et al., 2004).

3 Results

3.1 Ion concentrations and sources

- 20 Table 2 shows median concentrations for all ions measured in the cores. In addition, mean, maximum, minimum, and standard deviation (σ) are shown in Table S2, and box-plots of raw ion concentrations in the different cores are shown in Figure S1 in the Supplementary material.

- In general, median concentrations in the KM core are higher than in the other ice-rises cores, e.g. six to eight-fold higher concentrations of Na^+ , K^+ , Mg^{2+} and Cl^- in the KM core than in the KC core (which is further inland than the other sites) are found for the period 1995–2012. The relatively high Na^+ and Cl^- concentrations observed in the KM core are also detected in the upper meters of the S100 core (in the periods 1995–2000, and 1950–2000, respectively, Table 2). Similarly high values have been reported in several snow and firn samples from other western DML coastal sites (Kärkäs et al., 2005), and in Mill Island, Wilkes Land (Inoue et al., 2017). We found no significant relationship between median annual ion concentration and latitude, site elevation, and distance from the sea for most of the species, with the exception of annual SO_4^{2-} and annual MSA concentrations which show a significant decrease (at the 95 % confidence level) with latitude, and east longitude, respectively. However, additional ice cores from Fimbul are needed to obtain a robust conclusion on spatial distribution of major ions.

In order to assess the most important sources explaining the total variance in the glacio-chemical records from FIS, a principal component analysis (PCA) was applied to the different ion series measured in the KC, KM, BI, and S100 cores. Years in which no sub-annual concentrations were available in the S100 (1793, 1841, 1866, 1918, and 1944) due to low resolution, were filled in by linearly interpolating between the annual means of the previous and following year. For the PCA analysis, the logarithms of the raw concentrations were used, at sub-annual (using the raw values as input) and annual resolutions, and standardized by subtracting the mean of the data series from each data point and then dividing the result by the standard deviation of the data series. Due to the sampling resolution, only the KM and BI cores were comparable at a sub-annual level. PCA analyses were performed for three different periods of the S100 core: for the entire time interval spanning 1737–2000, for the subsection between 1737–1949, and between 1950–2000.

The sum of the variances of the first three principal components (PC1, PC2 and PC3) was $\geq 80\%$ of the total variance of the original sub-annual and annual data in all cores. Since the results of the sub-annual and annual PCA analysis are similar only the annual results are considered. The loadings of the first three (KC) and two (KM, BI, and S100) principal components are shown in Table 3. PCA results are consistent between the different cores. Consequently, the ions can be separated in two main groups: sea-salts species (Na^+ , Cl^- , K^+ , Mg^{2+} , and Ca^{2+}) and marine-biogenic/mixed (MSA, SO_4^{2-} , including NO_3^-) (Table 3). Generally, our results indicate that the major sources of ions at the different sites are the same, independent of the core site and mean concentrations of ions in the cores. Only at the KC site the PCA results imply an additional input of Ca^{2+} from other sources than sea-salt, as for instance mineral dust. Table 3 shows high loadings of NO_3^- and MSA in PC2, and thus, coherence between both species. This correspondence has been previously observed in an ice core from Lomonosovfonna, Svalbard, and a fertilizing effect was proposed as explanation for those findings (Wendl et al., 2015). Wendl et al. (2015) suggest that enhanced atmospheric NO_3^- concentrations and the corresponding nitrogen input to the ocean can trigger the growth of dimethyl-sulfide-(DMS)-producing phytoplankton. However, there is a variety of possible NO_3^- sources to polar sites, and the relative importance of these sources at certain locations and time is still in discussion (Mulvaney and Wolff, 1993; Savarino et al., 2007; Wolff et al. 2008; Weller et al. 2011; Pasteris et al., 2014; Sofen et al. 2014).

3.2 Long-term variability of ion concentrations

We use the two longest available records for FIS (KC and S100) to explore the long-term temporal variability of major ions, with special focus on sea-salts, represented by Cl^- and Na^+ (Figure 2). In the S100 core, Na^+ , Cl^- , K^+ , and Mg^{2+} median concentrations show a marked six-fold increase after the 1950s. However, there is no significant increase of the concentration of these species in the KC core. Due to its limited time coverage it cannot be determined if there was a substantial relative increase in concentrations at this site after the 1950s. MSA and NO_3^- concentrations do not show such marked increase in the S100 core and values agree between both cores after the 1950s (Figure S2 in the Supplementary material). Consequently, three periods can be distinguished in the S100 record: (i) the period between 1995–2000, comparable to the time covered by the KM

and BI cores; (ii) the period between 1737–1949, where ion concentrations remain low; and, (iii) the period between 1950–2000, where sea-salt concentrations increased (Table 2 and Table S2).

With the exception of MSA, all ions show a positive trend (significant at the 95 % confidence level) during the period 1950–2000, although the slope for NO_3^- is three orders of magnitude smaller than for the other ions. Such significant linear trend was not observed in the KC ion record over the same period (slope and error of the linear regression are shown in Table S3). Ions, with the exception of MSA, also show a positive and significant trend between 1737–1949 (Table S3), however, the increase is less marked than during the 1950–2000 period.

3.3 Sub-annual variability of ion concentrations

The lack of extensive precipitation measurements at sub-annual resolution near the sampling sites at FIS, makes a precise reconstruction of the precipitation regime at the area difficult. To obtain a time scale for the KC, KM, and BI ice-rises cores, Vega et al. (2016) employed $\delta^{18}\text{O}$ winter minima and summer maxima, and assumed uniform precipitation throughout the year at the core sites. The assumption was made on the basis of precipitation data for DML reported by Schlosser et al. (2008), which showed high temporal variability in the monthly sums due to the influence of cyclone activity affecting both, coastal and inland regions. In addition, at Neumayer station (70° 39' S, 8° 15' W), the closest to the ice-rises core sites, two precipitation maxima (April and October) are identifiable for the period 2001–2006, a manifestation of the semi-annual oscillation of the circumpolar trough (Schlosser et al., 2008). Considering the above, to investigate the sub-annual variability of the different ion groups in the KM, BI, and S100 cores, we associated the winter minima and summer maxima in $\delta^{18}\text{O}$ determined in the KC, KM, and BI cores (Vega et al., 2016), and in the S100 core (Kaczmarek et al., 2004), with the months of July and January, respectively. The values for April and October were derived by interpolation between January–July, and July–January, respectively, in each core time scale. We defined *summer samples*, as samples within November and April (NDJFMA), and *winter samples*, as samples within May and October (MJJASO). Summer and winter mean concentrations were then calculated based on logarithms of raw ion concentrations expressed in $\mu\text{mol L}^{-1}$. Ion concentrations were not available at the top 2 m (removed before drilling), therefore, the composite year consisted of 16 (1996–2011) and 15 (1997–2011) complete years for the KM and BI cores, respectively. In the S100 core, sub-annual variability were investigated only during the period 1995–2000, where the concentrations have sufficient temporal resolution. The resulting summer and winter mean concentrations in the cores are presented in Figure 3.

Sea-salt species (Na^+ and Cl^- , Figure 3a) show lower concentrations during summer in the BI, and S100 core, whereas in the KM core summer and winter show similar means. Both Mg^{2+} and Ca^{2+} (Figure 3b) show similar means in both summer and winter. MSA concentrations (Figure 3c) show summer maxima in all three cores, with a higher summer to winter difference in the BI core, compared with the KM, and S100 cores. These summer maxima are in agreement with the main source of MSA (marine-biogenic), most active during the warmer months. The MSA winter minimum is not as pronounced in the KM core as

in the BI core, while the lowest MSA minimum is reached in the S100 core. NO_3^- and SO_4^{2-} concentrations (Figure 3d) show a distinct increase toward the summer in the BI core, which is also observed in the KM core, although less marked. KM, and BI SO_4^{2-} concentrations are higher in the summer, while both NO_3^- and SO_4^{2-} summer and winter means are similar in the S100 core.

5 3.4 Sea-salt and non-sea-salt fractions

PCA results presented in section 3.1 show two main groups in which ions can be separated: sea-salts (ss-fraction), and marine biogenic/mixed (nss-fraction). In order to confirm the common sea-salt source for Na^+ and Cl^- , we calculated the Cl^-/Na^+ ratio, and ion sea-salt and non-sea-salt fractions. Table 4 shows median Cl^-/Na^+ ratios (using concentrations in $\mu\text{mol L}^{-1}$) in the KC, KM, BI, and S100 cores. Medians of the Cl^-/Na^+ ratio in the ice-rises cores are equal (KC, and BI) or slightly higher (KM) than the expected ratio in seawater (i.e., $\text{Cl}^-/\text{Na}^+ = 1.2$), while Cl^-/Na^+ medians in the S100 core are lower than the expected ratio in seawater, both before and after 1950. Maxima in the Cl^-/Na^+ ratio vary between 1.5–3.8, and minima between 0.1–0.9 (Table S4). These results show a clear difference in the Cl^-/Na^+ ratio between the ice-rises cores and the S100 core, i.e. a Cl^- to Na^+ imbalance in the S100 core associated to an excess of Na^+ . This excess of Na^+ can be due to the recombination of biogenic SO_4^{2-} with ssNa^+ , and/or to additional nss Na^+ sources (Legrand and Delmas, 1988). This imbalance can further be enhanced by a depletion of Cl^- due to shorter sea-salt atmospheric residence time, and HCl loss from snow (Legrand and Delmas, 1988; Wagon et al., 1999). HCl loss becomes significant at relatively low snow accumulation rates (Röthlisberger et al., 2003; Benassai et al., 2005), below the accumulation rate reported for the S100 site, therefore, it is unlikely that HCl loss is a dominant factor that could account for the low Cl^-/Na^+ ratios at this site. Cl^- depletion by recombination of ssCl^- with atmospheric acids is dependent on the acidic condition of the atmosphere, especially sulfuric acid (H_2SO_4), linked to marine biogenic emissions. Due to the seasonality of biogenic sulphur, the Cl^-/Na^+ ratio would present lower values during the summer months compared to the winter season (Jourdain and Legrand, 2002). Sub-annual Cl^-/Na^+ ratios (estimated as explained in section 3.3) in the S100 core show values of 1.4 ± 0.5 for the winter period, and 1.2 ± 0.1 for the summer period. Since the temporal resolution of the S100 core only allows sub-annual values for the period 1995–2000, is not possible to assess a sub-annual pattern on the Cl^-/Na^+ ratio, and Cl^- depletion by acidification cannot be ruled out as mechanism to explain the low ratios registered in the S100 core during the last centuries. In addition to Cl^- loss, low Cl^-/Na^+ ratios can also be a product of excess Na^+ from non-sea-salt sources (nss Na^+), as for example crustal material from snow-free coastal areas, nunataks, or dust transported from other continents. Table 4 shows the ssNa^+ , nss Na^+ (calculated as explained in section 2.3) and percentage of mean nss Na^+ to mean total Na^+ in the different cores. Since some of the calculated ssNa^+ values in the KC core were negative (5 % of the values), ssNa^+ statistics in Table 4 and Table S4 are shown considering all data points, and only positive ssNa^+ values. The KC core presents the largest contribution of nss Na^+ to total Na^+ with a 19 % in comparison to the KM, BI, and

S100 cores (0.6 %, 1.4 %, and 0.5 %, respectively), which is in agreement with PC3 in Table 3 pointing to a strong source of Ca^{2+} to the KC site.

As mentioned in section 2.3, we used the ssNa^+ fraction to calculate nss- and ss-fractions for Cl^- , SO_4^{2-} , K^+ , and Mg^{2+} , while ssCa^{2+} and nssCa^{2+} were obtained using the equations system described in section 2.3. Table 5 shows median concentrations of ss- and nss-fractions for Cl^- , SO_4^{2-} , K^+ , and Mg^{2+} , and Ca^{2+} , while ssNa^+ and nssNa^+ median concentrations are shown in Table 4. Complementary statistics are shown in Table S4 and Table S5. The sea-salt fraction clearly dominates in all ions, with the exception of SO_4^{2-} in the KC core, which shows almost three times more nssSO_4^{2-} than ssSO_4^{2-} . Nss-fractions often have negative values which can be associated to an ssNa^+ enrichment or to a depletion of major ions found in snow in comparison to bulk seawater, i.e. ion fractionation. Negative nss-fractions represent a higher percentage of total values at the S100 core compared to the ice-rises cores, with values up to 93 % for the S100 (1950–2000) (for nssCl^-), and up to 51 % for the BI core (for nssMg^{2+}).

3.5 Evidence for increased fractionated nss- SO_4^{2-} after 1950s

The nssSO_4^{2-} fraction contains all SO_4^{2-} sources besides sea-salts, e.g. marine biogenic emissions, and volcanic emissions. In coastal regions, most of the nssSO_4^{2-} can be attributed to marine biogenic activity via DMS oxidation (Legrand et al., 1992) with maxima in concentrations during the summer (Minikin et al., 1998). To evaluate if ion fractionation is evidenced in the core records, i.e. the snow is strongly depleted in ssSO_4^{2-} relative to ssNa^+ (Rankin and Wolff, 2002), leading to an underestimation of nssSO_4^{2-} , it is necessary to account for the biogenic contribution to total nssSO_4^{2-} at each core. In sites where biogenic SO_4^{2-} production is high, this fraction could mask a ssSO_4^{2-} depletion. Legrand and Pasteur (1998) have estimated $\text{MSA}/\text{nssSO}_4^{2-}$ ratios of 0.18 (annual), 0.29 (summer), and 0.86 (winter) (with concentration in $\mu\text{mol L}^{-1}$) in aerosol collected at Neumayer station, Antarctica. Median $\text{MSA}/\text{nssSO}_4^{2-}$ ratios calculated in the KC, KM, BI, and S100 cores (Table 6; complementary statistics are shown in Table S6) span a range between 0 and 0.3, therefore, closer to the annual and summer values reported by Legrand and Pasteur (1998). Using an annual $\text{MSA}/\text{nssSO}_4^{2-}$ ratio of 0.18 (Legrand and Pasteur, 1998) and the MSA concentrations measured in the KC, KM, BI, and S100 cores, we estimated the biogenic portion of nssSO_4^{2-} (bio-nssSO_4^{2-}) in all the cores to assess the percentage of mean bio-nssSO_4^{2-} to mean total SO_4^{2-} (Table 6). In the BI core, the estimation of bio-nssSO_4^{2-} surpasses the total SO_4^{2-} observed in the core, while in the KC, and KM cores the bio-nssSO_4^{2-} would represent about 58 % and 46 % of total SO_4^{2-} , respectively. These high percentages were expected especially in the KC core in which the nssSO_4^{2-} fraction dominates over ssSO_4^{2-} (section 3.4). In the S100 core, bio-nssSO_4^{2-} varies according to the time period considered with percentages three times higher during the period 1737–1749 (72 %), than the period 1950–2000 (24 %). It is important to bear in mind the estimation of bio-nssSO_4^{2-} when assessing the possible effect of fractionated aerosols as a source of sea-salts to the snow. In the ice-rises cores, the high estimated bio-nssSO_4^{2-} percentages would most likely mask any ssSO_4^{2-} depletion in sea-salt aerosols, making fractionation hard to evidence; consequently, fewer negative

nssSO₄²⁻ values or the absence of them in the ice-rises cores would not directly indicate that there is no input of fractionated sea-salts to the sites but rather reflect the dominance of the bio-nssSO₄²⁻ fraction in these sites. In the S100 core, this could be relevant for the pre-1950 period in which estimated bio-nssSO₄²⁻ accounts for 72 % of total SO₄²⁻.

In order to evaluate the possible effect of fractionated aerosols as a source of sea-salts to the snow on FIS, we use the calculated nssSO₄²⁻ fraction (section 2.3). The percentage of mean nssSO₄²⁻ relative to mean total SO₄²⁻ is one and a half- to three-times higher in the KC core than in the other ice-rises cores, KM and BI. Negative median nssSO₄²⁻ values were obtained in the S100 core, with negative nssSO₄²⁻ values being more pronounced after the 1950s (Table 5). These negative values found in the snow, i.e. the sea-salt content in snow is strongly depleted in ssSO₄²⁻ relative to seawater composition, suggest a possible role of frost flowers and wind-blown salty snow as source of sea-salts (Rankin and Wolff, 2002) to the S100 core (Figure 4a y b, black line). To assess the degree of fractionation of ssSO₄²⁻ in the cores in respect to seawater, we obtained the linear regression between annual nssSO₄²⁻ (both positive and negative nssSO₄²⁻ data points) and annual ssNa⁺ for the periods 1737–2000, 1737–1949, and 1950–2000, using a robust regression method (i.e. a method that gives a weight to each data point by using an iteratively reweighted least squares; we used the function *fitlm* with the *RobustOpts* option in the software Matlab) that is known to be less sensitive to a possible heteroscedasticity and non-Gaussianity of the model residuals (which is a common problem for ion concentration data) than the usual least squares method. We obtained negative slope values of 0.04, 0.03, and 0.04 for the 1737–2000, 1737–1949, and 1950–2000 periods, respectively. Figure 5 shows a scatter plot of annual nssSO₄²⁻ vs. ssNa⁺ for the 1737–2000 period. Following the approach by Wagenbach et al. (1998), we calculated corrected k_{seawater} values (k') by subtracting the absolute value of the linear regression slope from the constant $k_{\text{seawater}} = \frac{[\text{SO}_4^{2-}]}{[\text{Na}^+]}$ in seawater (Table S1), i.e. $k'_{1737-2000} = 0.02$, $k'_{1737-1949} = 0.03$, and $k'_{1950-2000} = 0.02$. The k' values recalculated for the S100 core are lower than k' values described by Palmer et al. (2002), and Plummer et al. (2012) at Law Dome ($k'_{\text{Law Dome}} = 0.04$, with concentrations expressed in $\mu\text{mol L}^{-1}$), and similar to the k' value obtained by Inoue et al. (2017) for a Mill Island coastal core ($k'_{\text{Mill Island}} = 0.03$, with concentrations expressed in $\mu\text{mol L}^{-1}$). Wagebach et al. (1998) reported winter k' of 0.02 (with concentrations expressed in $\mu\text{mol L}^{-1}$) associated to airborne sea-salt particles experiencing ssSO₄²⁻ depletion in respect to seawater, with a depletion factor ($k = k/k'$) of 5.5 for a firn core drilled at eastern Ronne Ice Shelf. The S100 core presents depletion factors of two for the period 1737–1949, and three for the period 1950–2000. The annual nssSO₄²⁻ fraction, without the effect of sulfate fractionation, was then recalculated in the S100 core using the values for k' of 0.02 and 0.03 (Table 7, and Figure 4a y b, red and blue lines, respectively).

4 Discussion

From the spatial and temporal variability of sea-salt concentrations in the different FIS cores discussed here, it was found that several mechanisms are contributing to the load of sea-salts at FIS, in agreement with the findings by Abram et al. (2013). The ice core data from S100 also suggest that there was a change in sea-salt deposition regime after the 1950s evidenced by an increase, up to six-fold, of median sea-salt concentrations after the 1950s in comparison with the previous 200 years. Although

a negative trend in SMB has been observed in the S100 and KC cores for the second half of the 20th century (Figure 2e and f) (Vega et al., 2016), the 0.2 % m w.e. y^{-1} decrease in accumulation registered in the S100 core after 1950 (Table S3) cannot account for the increase observed in sea-salt concentrations after 1950s. This increase in concentration is accompanied by a clear shift in $nssSO_4^{2-}$ toward negative values, indicative of $ssSO_4^{2-}$ depletion in sea-salts measured in the core in comparison to bulk seawater, with $ssSO_4^{2-}$ depletion factors of two for the period 1737–1949, and three for the period 1950–2000.

The negative $nssSO_4^{2-}$ values found in the FIS records could be explained by an enhanced input of sea-salts from (i) windblown frost flowers and/or (ii) aerosol formed after fractionated salty-snow sublimation, with both (i) and (ii) being formed in the neighbouring waters at the eastern flank of FIS. Yang et al. (2008) have reported that aerosol production via (ii) can be more than one-fold larger per unit area than sea-salt production from the open ocean. There is no or very limited amount of multi-annual sea ice near FIS, and young sea ice formed during winter in the vicinity of the S100 site is quickly covered by snow due to cyclonic activity. Trajectory studies of air with high sea-salt concentrations and low SO_4^{2-}/Na^+ ratios arriving at Halley station, showed that these air masses mainly originate at regions where young sea ice and frost flowers are formed (Hall and Wolff, 1998; Rankin and Wolff, 2002). However, conditions at Halley are not comparable to FIS, since the main easterly or north-northeasterly wind direction prevailing at Halley means an off-land air flow, thus creation of polynyas with open water and consecutive new ice formation, whereas at FIS, and most of the Dronning Maud Land coast, the wind is mainly parallel to the coast or even slightly towards the coast. In particular, a quantification of the areas covered by frost flowers is still missing. It is possible that those areas are comparatively small due to the generally high wind speeds prevailing above the Southern Ocean, resulting in a high percentage of frazil ice, and synoptic conditions lead to the quick development of a snow cover on the young sea ice. Although it is not possible to apportion the contribution of fractionated sea-salts via (i) or (ii) with the current data, it is plausible that a larger contribution of fractionated aerosol formed from salty-snow than by frost flowers, based on recent experimental evidence that frost flowers would not be a direct source of sea-salt aerosols (Yang et al., 2017). In addition, frequent stormy conditions in the area are detrimental for the formation of frost flowers, which form under quiet, undisturbed conditions, usually only in leads or small polynyas under the influence of anticyclonic weather. This also means low wind speeds and thus not much transport of frost flowers to the sampling sites at FIS. Thus, mechanism (ii), blowing salty snow formed on thin sea ice that sublimates during transport to form sea-salt aerosols, appears to be a much more probable explanation considering the local meteorological conditions in the study area.

Considering that we found no correlation between ion concentrations and site elevation, a decrease in wind transport efficiency of frost flowers (size of 10–20 mm) and aerosol formed via (ii) (size $>0.95 \mu m$) (Seguin et al., 2014) due to increased elevation cannot be addressed to explain the lower sea-salt values observed at the ice-rises compared to the S100 site. Local effects on annual SMB due to topography and meteorology at the KM and BI sites reported by Vega et al. (2016) are most likely involved in the different load of sea-salt to these sites.

The dramatic increase in fractionated sea-salt in the S100 core after the 1950s could be associated with a greater exposure of the S100 site to primary aerosol, in addition to an enhanced production of fractionated aerosol, evidenced by a dominance of

negative nssSO_4^{2-} values after 1950. Figures 2a and c show that sea-salts started to increase after 1950 with a marked peak corresponding to the year 1966 (± 3 years). According to Rignot et al. (2011), ice velocities near S100 were in the order of 100 m y^{-1} for the period 2007–2009, therefore, the S100 site has moved at least 5 km closer to the ice front between 1950 and 2000. In addition, as can be seen in the FIS contours shown in Figure 1, by 1963 the ice front in the vicinity of the S100 site was located about 17 km further north than its present position. As a consequence, the distance from the S100 site to open water would have changed through time and this would likely caused a greater input of sea-spray to the S100 site by shortening the distance to the open sea. However, sea-spray enhancing alone cannot account for the increase of sea-salt concentrations and the negative nssSO_4^{2-} found in the S100 samples. We hypothesize that the calving of Trolltunga, which occurred in 1967 (Vinje, 1975) (Figure 1), modified the sea ice conditions north of the S100 coring site, enhancing the input of fractionated sea-salts which then caused the marked sea-salt peak appearing in 1966 (± 3 years). Furthermore, additional support for an effect of the Trolltunga calving event is the fact that negative nssSO_4^{2-} slowly decreased between 1950–1966, showing a marked minimum around 1966 (± 3 years) (Figure 4b). The much extended Trolltunga which was present before the calving event would have formed a larger bay to the east, favourable for a higher concentration of sea ice caused by the prevailing easterly winds, resulting in both thicker and longer-lasting sea ice which would limit sea-spray formation. Such thick sea ice does not seem to form under post-calving event conditions, e.g. with a shorter tongue. In order to explain the fractionated sea-salt values detected in the S100 core, there must be an enhanced source of fractionated sea-salts after the calving event. This would be the case if young sea ice (where fractionation of sea-salts can take place) formed near the S100 site as a result of the greater area of open sea available after the calving event. Thicker, long-lasting sea ice present before the calving event would have been a more stable substrate, prone to less flooding through cracks and leads, and would also likely have reduced salinity content in the snow compared to young sea ice (Massom et al., 2001). Considering the conjecture by Rhodes et al. (2017), i.e. that young sea ice is more saline than multi-year ice, it can be expected that sea-salt aerosols produced by blowing snow over sea ice would have higher sea-salt concentrations when young-ice is formed than when multi-year sea ice is formed, in coherence with the proposed hypothesis. The higher sea-salt concentrations and the negative nssSO_4^{2-} values found in S100 after the Trolltunga calving, could thus be explained by a combination of shortening the distance from the S100 site to the ice shelf front, and an enhanced contribution of sea-salt aerosols entrained by blowing salty snow found over young sea ice formed near the S100 site. If the air is unsaturated, water in these snow particles will sublimate producing fractionated sea-salt aerosol. As schematized in Figure 2 in Rhodes et al. (2017), the sea-salt aerosol can be transported inland and be deposited either by dry or wet deposition. Since sea-salt concentrations are much higher at the S100 core than in the ice-rises cores, it is plausible that most of the flux of sea-salts at the S100 site is due to dry deposition, due to the short distance from the coast and low elevation, while deposition at the ice-rises would be balanced between the wet and dry regimes. Rhodes et al. (2017) found a marked gradient in the ratio between sea ice sea-salts and oceanic sea-salts (produced by bubble bursting) with distance to the source, in Arctic sites, with higher ratios closer to the sea ice source and when the sample location is in the path between sea ice and prevailing winds. To test the hypothesis presented here, a closer analysis of satellite and historical sea ice data and a model-

based study to estimate the spatial and elevation gradient of sea ice sea-salts to FIS can be done, which, however, is beyond the scope of the present study.

Other possible mechanisms, such as deposition of sea-salts with rime or windblown snow present over multi-annual sea ice, can explain neither the increase in sea salt concentration nor the fractionation observed in S100 after the 1950s. Additionally, annual averages of monthly zonal and meridional wind speeds (ERA40, Uppala et al., 2005) for the area (69°S–71°S, 3.5°W–5°E) between 1955–2001 (Figure 6) show no significant positive trends, thus evidencing that the S100 sea-salt increase after 1950s cannot be related to enhanced transport by wind.

Due to the limited time coverage of the KC, KM, and BI cores, we do not know whether there was a relative increase in sea-salt concentrations in the ice-rises cores after the 1950s influenced by the Trolltunga calving. Due to the large input of bio-nssSO₄²⁻ to the ice-rises sites, any possible signal of fractionated sea-salts in any of the ice-rises cores could be easily masked by the biogenic fraction (e.g. no significant negative nssSO₄²⁻ values would be observed). Relatively higher sea-salt concentrations measured in the KM core in comparison to the other ice-rises cores could be explained by a combination of distance to the sea and the prevailing precipitation and wind conditions in the area: precipitation on FIS is mainly caused by frontal systems of cyclones in the circumpolar trough that move eastwards north of the coast, thus leading to easterly or east-north-easterly surface winds on FIS (Schlosser et al., 2008). This means that even though BI is equally close to the sea as KM (Figure 1), KM has by far the shortest distance to the source of marine aerosols of all three ice-rises cores, which could explain the comparatively high sea-salt concentrations (Table 2).

5 Conclusions

This study reports sub-annual and long-term temporal sea-salt and major ion concentration changes measured in three recently drilled firn cores from different ice-rises located at Fimbul Ice Shelf (FIS): Kupol Ciolkovskogo, Kupol Moskovskij, and Blåskimen Island, and a 100 m long core drilled near the FIS edge (S100). A significant increase in sea-salts is observed in the S100 core after the 1950s, which is associated with an enhanced exposure of the S100 site to primary sea-salt aerosol associated with a shorter distance from the S100 site to the ice front during the last decades, and an enhanced input of fractionated sea-salts. This increase in sea-salt concentrations was accompanied by a shift in nssSO₄²⁻ toward negative values, which suggests input of fractionated sea-salts to the ion load in the S100 core most likely by enhanced sea-salts production by blowing salty snow over sea ice. Due to the large input of bio-nssSO₄²⁻ to the ice-rises cores, it is hard to assess the degree of ssSO₄²⁻ depletion in snow in comparison to bulk seawater at these sites. Consequently, the results of this study suggest that the S100 record contains a sea-salt record dominated by processes of sea ice formation in the neighbouring waters, and a strong component associated to the concentration gradient between the S100 site and the FIS edge. In contrast, the ice-rises cores record the signal of larger-scale conditions of atmospheric flow, large inputs of bio-nssSO₄²⁻, and less efficient transport of sea-salts evidenced by lower median concentrations than at the S100 site. These findings are of vital importance for the

understanding of the mechanisms of sea-salt aerosol production, transport and deposition at coastal Antarctic sites, and for the improvement of the current Antarctic sea ice reconstructions based on sea-salt chemical proxies.

6 Data availability

5 For the chemistry profiles of the KC, KM, BI, and S100 cores, please download the data from Pangaea (<https://doi.pangaea.de/10.1594/PANGAEA.889018>).

MODIS Mosaic of Antarctica (MOA) image is available through the GIS package Quantarctica, version 2.0 at <http://quantarctica.npolar.no/>.

ERA40 reanalysis data is available at <https://climatedataguide.ucar.edu/climate-data/era40> (Uppala, et al., 2005).

Acknowledgements

10 We are grateful to those who helped to collect, transport, sample and analyse the firn cores from FIS. We would like to thank V. Goel, J. Kohler, and J. van Oostveen for providing the 50-m contours and the pre-calving extent of Trolltunga, respectively, used in Figure 1, and T. Maldonado for processing the data for Figure 6. In addition, we thank the two anonymous referees for their thorough and constructive revision of the manuscript. We thank the Norwegian Polar Institute's team behind the Quantarctica package. Financial support came from Norwegian Research Council through NARE and the Centre for Ice,
15 Climate and Ecosystems (ICE) at the Norwegian Polar Institute in Tromsø. Additional support was received from University of Costa Rica, network ISONet (project B6-774).

References

- Abram, N. J., Wolff, E. W., and Curran, M. A. J.: A review of sea ice proxy information from polar ice cores, *Quat. Sci. Rev.*, 79, doi:10.1016/j.quascirev.2013.01.011, 2013.
- Benassai, S., Becagli, S., Gragnani, R., Magand, O., Proposito, M., Ilaria, F., Traversi, R., and Udisti, R.: Sea-spray deposition in Antarctic coastal and plateau areas from ITASE traverses, *Ann. Glaciol.*, 41, 32–40, 2005.
- Curran, M., van Ommen, T., and Morgan, V.: Seasonal characteristics of the major ions in the high-accumulation dome Summit South ice core, Law Dome, Antarctica, *Ann. Glaciol.*, 27, 385–390, 1998.
- Divine, D.V., Isaksson, E., Kaczmarska, M., Godtlibsen, F., Oerter, H., Schlosser, E., Johnsen, S.J., van den Broeke, M. and van de Wal, R.S.W.: Tropical Pacific - High Latitude South Atlantic Teleconnections as Seen in the $\delta^{18}\text{O}$ Variability in Antarctic Coastal Ice Cores, *J. Geophys. Res.*, 114, D11112, doi:10.1029/2008JD010475, 2009.
- Dominé, F., Sparapani, R., Ianniello, A., and Beine, H. J.: The origin of sea salt in snow on arctic sea ice and in coastal regions, *Atmos. Chem. Phys.*, 4, 2259–2271, 2004.
- Fischer, H., Siggaard-Andersen, M. -L., Ruth, U., Röthlisberger, R., and Wolff, E.: Glacial/interglacial changes in mineral dust and sea-salt records in polar ice cores: Sources, transport and deposition, *Rev. Geophys.*, 45, RG1002, doi:10.1029/2005RG000192, 2007.
- Goel, V. Brown, and J. Matsuoka, K. Glaciological Settings and recent mass balance of the Blåskimen Island in Dronning Maud Land, Antarctica. *The Cryosphere*, 11, 2883–2896, 2017.
- Hall, J.S., and Wolff, E.W.: Causes of seasonal and daily variations in aerosol seasalt concentrations at a coastal Antarctic station. *Atmospheric Environment*, 32(21), 3669e3677. [http://dx.doi.org/10.1016/s1352-2310\(98\)00090-9](http://dx.doi.org/10.1016/s1352-2310(98)00090-9), 1998.
- Huang, J., and Jaeglé, L.: Wintertime enhancements of sea salt aerosol in polar regions consistent with a sea ice source from blowing snow, *Atmos. Chem. Phys.*, 17, 3699–3712, doi:10.5194/acp-17-3699-2017, 2017.
- Inoue, M., Curran, M. A. J., Moy, A. D., van Ommen, T. D., Fraser, A. D., Phillips, H. E., and Goodwin, I. D.: A glaciochemical study of 120 m ice core from Mill Island, East Antarctica, *Clim. Past*, 13, 437-453, doi:10.5194/cp-13-437-2017, 2017.
- Isaksson, E. and Melvold, K.: Trends and patterns in the recent accumulation and oxygen isotopes in coastal Dronning Maud Land, Antarctica: interpretations from shallow ice cores, *Ann. Glaciol.*, 35, 175–180, 2002.
- Jourdain, B. and Legrand, M.: Year-round records of bulk and size- segregated aerosol composition and HCl and HNO₃ levels in the Dumont d'Urville (coastal Antarctica) atmosphere: Implications for sea-salt aerosol fractionation in the winter and summer, *J. Geophys. Res.*, 107, 4645, doi:10.1029/2002JD002471, 2002.
- Jourdain, B., S. Preunkert, O. Cerri, H. Castebrunet, R. Udisti, and Legrand, M.: Year-round record of size-segregated aerosol composition in central Antarctica (Concordia station): Implications for the degree of fractionation of sea-salt particles, *J. Geophys. Res.*, 113, D14308, doi:10.1029/2007JD009584, 2008.

- Kaczmarska, M., Isaksson, E., Karlöf, L., Winther, J-G., Kohler, J., Godtlielsen, F., Ringstad Olsen, L., Hofstede, C. M., Van Den Broeke, M. R., Van De Wal, R. S.W., Gundestrup, N.: Accumulation variability derived from an ice core from coastal Dronning Maud Land, Antarctica, *Ann. Glaciol.* 39, 339–345, 2004.
- Kaczmarska, M., Isaksson, E., Karlöf, L., Brandt, O., Winther, J-G., Van De Wal, R., Van Den Broeke, M. R., Johnsen, S.:
5 Ice core melt features in relation to Antarctic coastal climate, *Antarc. Science*, 18(2), 271–278, 2006.
- Kreutz, K.J., Mayewski, P.A., Whitlow, S.I., and Twickler, M.S.: Limited migration of soluble ionic species in a Siple Dome, Antarctica, ice core. In: Budd, W.F. (Ed.), *Ann. Glaciol.*, 27, 371–377, 1998.
- Kärkäs, E., Martma, T., and Sonninen, E.: Physical properties and stratigraphy of surface snow in western Dronning Maud Land, Antarctica, *Polar Res.*, 24(1–2), 55–67, 2005.
- 10 Langley, K., Kohler, J., Sinisalo, A., Øyan, M. J., Hamran, S. E., Hattermann, T., Matsuoka, K., Nøst, O. A. and Isaksson E.: Low melt rates with seasonal variability at the base of Fimbul Ice Shelf, East Antarctica, revealed by in situ interferometric radar measurements, *Geophys. Res. Lett.*, 41, 8138–8146, doi:10.1002/2014GL061782, 2014.
- Legrand, M. R., and Delmas, R. J.: Formation of HCl in the Antarctic atmosphere, *Geophys. Res. Atmos.*, 93(D6), 7153–7168, 1988.
- 15 Legrand, M., Feniet-Saigne, C., Saltzman, E. S., and Germain, C.: Spatial and temporal variations of methanesulfonic acid and non sea salt sulfate in Antarctic ice, *J. Atmos. Chem.*, 14, 245–260, 1992.
- Legrand, M., and Pasteur, E. C.: Methane sulfonic acid to non-sea-salt sulfate ratio in coastal Antarctic aerosol and surface snow, *J. Geophys. Res.*, 103(D9), 10991–11006, 1998.
- Levine, J. G., Yang, X., Jones, A. E., and Wolff, E. W.: Sea salt as an ice core proxy for past sea ice extent: A process-based
20 model study, *J. Geophys. Res. Atmos.*, 119, 5737–5756, doi:10.1002/2013JD020925, 2014.
- Littot, G. C., Mulvaney, R., Röthlisberger, R., Udisti, R., Wolff, E. W., Castellano, E., De Angelis, M., Hansson, M. E., Sommer, S. and Steffensen, J. P.: Comparison of analytical methods used for measuring major ions in the EPICA Dome C (Antarctica) ice core, *Ann. Glaciol.*, 35, 299–305, 2002.
- Lunde, T.: On the snow accumulation in Dronning Maud Land. *Den Norske Antarktischspedisjonen 1956–60*, Scientific
25 Results No. 1. Norsk Polarinstitut Skriffter, No. 123, 1961.
- Lutgens, F. K., and Tarbuck, E. J.: *Essentials of Geology*, 11th Ed., Prentice Hall, 2012.
- Mahalinganathan, K., Thamban, M., Laluraj, C. M., and Redkar, B. L.: Relation between surface topography and sea-salt snow chemistry from Princess Elizabeth Land, East Antarctica, *The Cryosphere*, 6, 505–5015, 2012.
- Massom, R.A., Eicken, H., Haas, C., Jeffries, M.O., Drinkwater, M.R., Sturm, M., Worby, A.P., Wu, X.R., Lytle, V.I., Ushio,
30 S., Morris, K., Reid, P.A., Warren, S.G., Allison, I.: Snow on Antarctic sea ice, *Rev. Geophys.*, 39(3), 413–445. <http://dx.doi.org/10.1029/2000rg000085>, 2001.
- Matsuoka, K., Hindmarsh, R. C. A., Moholdt, G., Bentley, M. J., Pritchard, H. D., Brown, J., Conway, H., Drews, R., Durand, G., Goldberg, D., Hattermann, T., Kingslake, J., Lenaerts, J. T. M., Martín, C., Mulvaney, R., Nicholls, K., Pattyn, F., Ross,

- N., Scambos, T., and Whitehouse, P.: Antarctic ice rises and rumples: Their properties and significance for ice-sheet dynamics and evolution, *Earth Sci. Rev.*, 150, 724–745, 2015.
- Melvold, K.: Impact of recent climate on glacier mass balance: studies on Kongsvegen, Svalbard and Jutulstraumen, Antarctica, D.Sc. thesis, University of Oslo., Department of Geography Report 13, 1999.
- 5 Melvold, K., Hagen, J. O., Pinglot, J. F. and Gundestrup, N.: Large spatial variation in accumulation rate in Jutulstraumen ice stream, Dronning Maud Land, Antarctica, *Ann. Glaciol.*, 27, 231–238, 1998.
- Minikin, A., Legrand, M., Hall, J., Wagenbach, D., Kleefeld, C., Wolff, E., Pasteur, E. C., and Ducroz, F.: Sulfur-containing species (sulfate and methanesulfonate) in coastal Antarctic aerosol and precipitation, *J. Geophys. Res.*, 103(D9), 10975, 10975–10990, 1998.
- 10 Mulvaney, R., Coulson, G. F. J. and Corr, H. F. J.: The fractionation of sea salt and acids during transport across an Antarctic ice shelf, *Tellus*, 45B, 179–187, 1993.
- Mulvaney R., and Wolff, E. W.: Evidence for Winter/Spring Denitrification of the Stratosphere in the Nitrate Record of Antarctic Firn Cores, *J. Geophys. Res.*, 98(D3), 5213–5220, 1993.
- Neethling, D. C.: Snow accumulation on the Fimbul ice shelf, western Dronning Maud Land, Antarctica, International Association of Scientific Hydrology Publication 86 (Symposium at Hanover1968—Antarctic Glaciological Exploration (ISAGE)), 390–404, 1970.
- 15 Palmer, A. S., Morgan, V. I., Curran, M. A. J., van Ommen, T. D., and Mayewski, P. A.: Antarctic volcanic flux ratios from Law Dome ice cores, *Ann. Glaciol.*, 35, 329–332, doi:10.3189/172756402781816771, 2002.
- Pasteris, D. R., McConnell, J. R., Das, S. B., Criscitiello, A. S., Evans, M. J., Maselli, O. J., Sigl, M., and Layman, L.: Seasonally resolved ice core records from West Antarctica indicate a sea ice source of sea-salt aerosol and a biomass burning source of ammonium, *J. Geophys. Res. Atmos.*, 119, 9168–9182, doi:10.1002/2013JD020720, 2014.
- 20 Paterson, W. S. B.: *The Physics of Glaciers*, 3rd Edn., Butterworth-Heinemann, Burlington, 469 pp., 1994.
- Petit J.R., Jouzel J., Raynaud D., Barkov N.I., Barnola J.M., Basile, I., Bender, M., Chappellaz, J., Davis, M., Delaygue, G., Delmotte, M., Kotlyakov, V. M., Legrand, M., Lipenkov, V. Y., Lorius, C., Pépin, L., Ritz, C., Saltzman E., and Stievenard, M.: Climate and Atmospheric History of the Past 420,000 years from the Vostok Ice Core, Antarctica, *Nature*, 399, 429–436, 25 1999.
- Philippe, M., Tison, J.-L., Fjøsne, K., Hubbard, B., Kjaer, H. A., Lenaerts, J. T. M., Drews, R., Sheldon, S. G., De Bondt, K., Claey, P., and Pattyn, F.: Ice core evidence for a 20th century increase in surface mass balance in coastal Dronning Maud Land, East Antarctica, *The Cryosphere*, 10, 2501–2516, doi:10.5194/tc-10-2501-2016, 2016.
- 30 Plummer, C. T., Curran, M. A. J., van Ommen, T. D., Rasmussen, S. O., Moy, A. D., Vance, T. R., Clausen, H. B., Vinther, B. M., and Mayewski, P. A.: An independently dated 2000-yr volcanic record from Law Dome, East Antarctica, including a new perspective on the dating of the 1450s CE eruption of Kuwae, Vanuatu, *Clim. Past*, 8, 1929–1940, doi:10.5194/cp-8-1929-2012, 2012.

- Quantarctica, version 2.0, <http://quantarctica.npolar.no/>, last visited 2017-12-12.
- Rankin, A. M., Auld, V., and Wolff, E. W.: Frost flowers as a source of fractionated sea salt aerosol in the polar regions, *Geophys. Res. Lett.*, 27(21), 3469–3472, doi:10.1029/2000GL011771, 2000.
- Rankin, A. M. and Wolff, E. W.: Frost flowers: Implications for tropospheric chemistry and ice core interpretation, *J. Geophys. Res.*, 107(D23), 4683, doi:10.1029/2002JD002492, 2002.
- Rankin, A.M., and Wolff, E.W.: A year-long record of size-segregated aerosol composition at Halley, Antarctica, *J. Geophys. Res. Atmos.*, 108(D24), 4775, <http://dx.doi.org/10.1029/2003jd003993>, 2003.
- Rankin, A. M., Wolff, E. W., and Mulvaney, R.: A reinterpretation of sea-salt records in Greenland and Antarctic ice cores?, *Ann. Glaciol.*, 39, 276–282, doi:10.3189/172756404781814681, 2004.
- 10 Rhodes, R. H., Yang, X., Wolff, E. W., McConnell, J. R., and Frey, M. M.: Sea ice as source of sea salt aerosol to Greenland ice cores: a model-based study, *Atmos. Chem. Phys.*, 17, 9417–9433, <https://doi.org/10.5194/acp-17-9417-2017>, 2017.
- Rignot, E., Mouginot, J., and Scheuchl, B.: Ice flow of the Antarctic ice sheet, *Science*, 333, 1427–1430, 2011.
- Rolstad, C., Whillans, I. M., Hagen, J. O. and Isaksson, E.: Large-scale force budget of an outlet glacier: Jutulstraumen, Dronning Maud Land, East Antarctica, *Ann. Glaciol.*, 30(1), 35–41, 2000.
- 15 Roscoe, H. K., Brooks, B., Jackson, A. V., Smith, M.H., Walker, S. J., Obbard, R. W., and Wolff, E. W.: Frost flowers in the laboratory: Growth, characteristics, aerosol, and the underlying sea ice, *J. Geophys. Res.*, 116, D12301, doi:10.1029/2010JD015144, 2011.
- Röthlisberger, R., Mulvaney, R., Wolff, E., Hutterli, M., Bigler, M., De Angelis, M., Hansson, M., Steffensen, J. P., and Udisti, R.: Limited dechlorination of sea-salt aerosols during the last glacial period: Evidence from the European Project for Ice Coring in Antarctica (EPICA) Dome C ice core, *J. Geophys. Res.*, 108, 4526, doi:10.1029/2003jd003604, 2003.
- 20 Savarino, J., Kaiser, J., Morin, S., Sigman, D., Thieme, M.: Nitrogen and oxygen isotopic constraints on the origin of atmospheric nitrate in coastal Antarctica, *Atmos. Chem. Phys.*, 7, 1925–1945, 2007.
- Schlosser, E., Anshütz, H., Isaksson, I., Martma, T., Divine, D., and Nøst, O.-A.: Surface mass balance and stable oxygen isotope ratios from shallow firn cores on Fimbulisen, East Antarctica, *Ann. Glaciol.*, 53, 70–78, doi:10.3189/2012AoG60A102, 25 2012.
- Schlosser, E., Anshütz, H., Divine, D., Martma, T., Sinisalo, A., Altnau, S., and Isaksson, E., Recent climate tendencies on an East Antarctic ice shelf inferred from a shallow firn core network, *J. Geophys. Res. Atmos.*, 119, 6549–6562, 2014.
- Schlosser, E., Duda, M. G., Powers, J. G., and Manning, K. H.: The precipitation regime of Dronning Maud Land, Antarctica, derived from AMPS (Antarctic Mesoscale Prediction System) Archive Data, *J. Geophys. Res.*, 113, D24108, 30 doi:10.1029/2008JD009968, 2008.
- Seguin, A. M., Norman, A.-L., and Barrie, L.: Evidence of sea ice source in aerosol sulfate loading and size distribution in the Canadian High Arctic from isotopic analysis, *J. Geophys. Res. Atmos.*, 119(2), 1087–1096, doi:10.1002/2013JD020461, 2014.

- Sinisalo, A., Anschütz, H., Aasen, A. T., Langley, K., von Deschwanen, A., Kohler, J., Matsuoka, K., Hamran, S. E., Øyan, M. J., Schlosser, E., Hagen, J. O., Nøst, O. A., and Isaksson, E.: Surface mass balance on Fimbul ice shelf, East Antarctica: Comparison of field measurements and large-scale studies, *J. Geophys. Res. Atmos.*, 118(11), 625–11,635, doi:10.1002/jgrd.50875, 2013.
- 5 Sofen, E. D., Alexander, B., Steig, E. J., Thiemens, M. H., Kunasek, S. A., Amos, H. M., Schauer, A. J., Hastings, M. G., Bautista, J., Jackson, T. L., Vogel, L. E., McConnell, J. R., Pasteris, D. R., and Saltzman, E. S.: WAIS Divide ice core suggests sustained changes in the atmospheric formation pathways of sulfate and nitrate since the 19th century in the extratropical Southern Hemisphere, *Atmos. Chem. Phys.*, 14, 5749–5769, 2014.
- 10 Stenberg, M., Isaksson, E., Hansson, M., Karlén, W., Myewski, P. A., Twickler, M. S., Whitlow, S. I., and Gundestrup, N.: Spatial variability of snow chemistry in western Dronning Maud Land, Antarctica, *Ann. Glaciol.*, 27, 378–384, 1998.
- Stenni, B., Curran, M. A. J., Abram, N. J., Orsi, A., Goursaud, S., Masson-Delmotte, V., Neukom, R., Goosse, H., Divine, D., van Ommen, T., Steig, E. J., Dixon, D. A., Thomas, E. R., Bertler, N. A. N., Isaksson, E., Ekaykin, A., Frezzotti, M., and Werner, M.: Antarctic climate variability at regional and continental scales over the last 2,000 years, *Clim. Past*, 13, 1609–1634, <https://doi.org/10.5194/cp-13-1609-2017>, 2017.
- 15 Swithinbank, C.: Glaciology I: A, The morphology of the Ice Shelves of western Dronning Maud Land; B, The Regime of the Ice Shelves at Maudheim as shown by Stake Measurements. Norwegian-British-Swedish Antarctic Expedition, 1949–52. Scientific Results, Vol. III, 1957.
- Summerhayes, C. P., and Thorpe, S. A. *Oceanography: An Illustrated Guide*, Wiley, New York, Chapter 11, 165–181, 1996.
- 20 Thomas, E. R., van Wesseem, J. M., Roberts, J., Isaksson, E., Schlosser, E., Fudge, T., Vallelonga, P., Medley, B., Lenaerts, J., Bertler, N., van den Broeke, M. R., Dixon, D. A., Frezzotti, M., Stenni, B., Curran, M., and Ekaykin, A. A.: Regional Antarctic snow accumulation over the past 1000 years, *Clim. Past*, 13, 1491–1513, <https://doi.org/10.5194/cp-13-1491-2017>, 2017.
- Twickler, M., and Whitlow, S. Appendix B, in: *Guide for the collection and analysis of ITASE snow and firn samples*, edited by: Mayewski, P.A., and Goodwin, I.D., International Trans-Antarctic Scientific Expedition (ITASE), Bern, Past Global Changes (PAGES report 97-1), 1997.
- 25 Udisti, R., Dayan, U., Becagli, S., Busetto, M., Frosini, D., Legrand, M., Lucarelli, F., Preunkert, S., Severi, M., Traversi, R., and Vitale, V.: Sea spray aerosol in central Antarctica. Present atmospheric behaviour and implications for paleoclimatic reconstructions, *Atmos. Environ.*, 52, 109–120, 2012.
- 30 Uppala, S. M., Kållberg, P. W., Simmons, A. J., Andrae, U., Da Costa Bechtold, V., Fiorino, M., Gibson, J. K., Haseler, J., Hernandez, A., Kelly, G. A., Li, X., Onogi, K., Saarinen, S., Sokka, N., Allan, R. P., Andersson, E., Arpe, K., Balmaseda, M. A., Beljaars, A. C. M., Van De Berg, L., Bidlot, J., Bormann, N., Caires, S., Chevallier, F., Dethof, A., Dragosavac, M., Fisher, M., Fuentes, M., Hagemann, S., Hólm, E., Hoskins, B. J., Isaksen, L., Janssen, P. A. E. M., Jenne, R., McNally, A. P., Mahfouf, J.-F., Morcrette, J.-J., Rayner, N. A., Saunders, R. W., Simon, P., Sterl, A., Trenberth, K. E., Untch, A., Vasiljevic, D., Viterbo, P., and Woollen, J.: The ERA-40 Re-Analysis, *Quart. J. Roy. Meteor. Soc.*, 131, 2961–3012, doi:10.1256/qj.04.176, 2005.

- Vega, C. P., Schlosser, E., Divine, D. V., Kohler, J., Martma, T., Eichler, A., Schwikowski, M., and Isaksson, E.: Surface mass balance and water stable isotopes derived from firn cores on three ice rises, Fimbul Ice Shelf, Antarctica, *The Cryosphere*, 10, 2763–2777, doi:10.5194/tc-10-2763-2016, 2016.
- Vinje, T. E.: *Frift av Trolltunga i Weddellhavet*, Norsk Polarinstitutt. Arbok, 213 pp., 1975.
- 5 Wagenbach, D., Ducroz, F., Mulvaney, R., Keck, L., Minikin, A., Legrand, M., Hall, J. S., Wolff, E. W.: Sea-salt aerosol in coastal Antarctic regions, *J. Geophys. Res.*, 103, 10961–10974, 1998.
- Wagenbach, D., Graf, W., Minikin, A., Trefzer, U., Kipfstuhl, J., Oerter, H., and Blindow, N.: Reconnaissance of chemical and isotopic firn properties on top of Berkner-Island, Antarctica. In: Morris, E.M. (Ed.), *Ann. Glaciol.: Proceedings of the Fifth International Symposium on Antarctic Glaciology*, 20, 307–312, 1994.
- 10 Wagnon, P., Delmas, R. J., and Legrand, M.: Loss of volatile acid species from upper firn layers at Vostok, Antarctica, *J. Geophys. Res.*, 104, 3423–3431, 1999.
- Weller, R., and Wagenbach, D.: Year-round chemical aerosol records in continental Antarctica obtained by automatic sampling, *Tellus*, 59, 755–765, 2007.
- Weller, R., Wagenbach, D., Legrand, M., Elsässer, C., Tian-Kunze, X., and König-Langlo, G.: Continuous 25-yr aerosol records at coastal Antarctica– I: inter-annual variability of ionic compounds and links to climate indices, *Tellus*, 63B, 901–919, 2011.
- Wendl, I.: High resolution records of black carbon and other aerosol constituents from the Lomonosovfonna 2009 ice core, PhD Thesis, University of Bern, Switzerland, 2014.
- Wendl, I. A., Eichler, A., Isaksson, E., Martma, T., and Schwikowski, M.: 800-year ice-core record of nitrogen deposition in Svalbard linked to ocean productivity and biogenic emissions, *Atmos. Chem. Phys.*, 15, 7287–7300, doi:10.5194/acp-15-7287-2015, 2015.
- 20 Wolff, E. W., Jones, A. E., Bauguitte, S. J. B., and Salmon, R. A.: The interpretation of spikes and trends in concentration of nitrate in polar ice cores, based on evidence from snow and atmospheric measurements, *Atmos. Chem. Phys.*, 8, 5627–5634, 2008.
- 25 Yang, X., Neděla, V., Runštuk, J., Ondrušková, G., Krausko, J., Vetráková, L., and Heger, D.: Evaporating brine from frost flowers with electron microscopy and implications for atmospheric chemistry and sea-salt aerosol formation, *Atmos. Chem. Phys.*, 17, 6291–6303, doi:10.5194/acp-17-6291-2017, 2017.
- Yang, X., Pyle, J. A., and Cox, R. A.: Sea salt aerosol production and bromine release: Role of snow on sea ice, *Geophys. Res. Lett.*, 35(L16815), doi:10.1029/2008GL034536, 2008.
- 30 Yang, X., Pyle, J. A., Cox, R. A., Theys, N., and Van Roozendaal, M.: Snow-sourced bromine and its implications for polar tropospheric ozone, *Atmos. Chem. Phys.*, 10, 7763–7773, doi:10.5194/acp-10-7763-2010, 2010.

Tables

Table 1. Cores (KC, KM, BI, S100) locations and sampling details. Distances of the core locations to the ice shelf side were obtained using the GIS package Quantarctica (www.quantarctica.org). (*) refers to Kaczmarek et al. (2004), and (§) to Vega et al. (2016). SMB is Surface Mass Balance.

Site	Location	Elevation (m a.s.l.)	Core length <i>Ice depth</i> Ice temp. at 10 m (m)	Distance from the coast (km)	Time coverage (years)	Average SMB (m w.e. y ⁻¹)
KC§	70°31'S, 2°57'E	264	20.0 460 -17.5	42	(1958–2012) ± 3	0.24
KM§	70°8'S, 1°12'E	268	19.6 410 -15.9	12	(1995–2014) ± 1	0.68
BI§	70°24'S, 3°2'W	394	19.5 460 -16.1	10	(1996–2014) ± 1	0.70
S100*	70°14'S, 4°48'E	48	100 - -17.5	3	(1737–2000) ± 3	0.30

Table 2. Median ion concentrations (in $\mu\text{mol L}^{-1}$) in the KC, KM, BI, and S100 firn/ice cores. Ion concentrations at the top 2 m of the KC, KM, and BI cores were not measured. Non-detected concentrations were set as half the detection limit of each ion. Values of water stable isotopes and deuterium excess for the KC, KM, and BI are reported by Vega et al. (2016).

Site	Period (years)	MSA	Cl^-	NO_3^-	SO_4^{2-} ($\mu\text{mol L}^{-1}$)	Na^+	K^+	Mg^{2+}	Ca^{2+}
KC	1958–2007	0.2	10.0	0.6	1.8	9.4	0.2	0.9	0.5
KM	1995–2012	0.3	71.3	0.4	4.5	57.7	1.5	6.3	1.6
BI	1996–2012	0.4	23.1	0.4	1.9	19.0	0.5	2.0	0.6
S100	1737–2000	0.1	20.9	0.5	1.2	20.7	0.4	2.0	0.7
S100	1995–2000	0.1	132.4	0.6	3.2	144.0	3.3	10.7	3.0
S100	1737–1949	0.1	16.0	0.6	1.0	15.1	0.3	1.4	0.5
S100	1950–2000	0.1	88.5	0.5	2.8	98.2	2.0	7.9	1.9

Table 3. PCA loadings of the first three (KC) and two (KM, BI, and S100) principal components calculated at an annual resolution in a set of 8 different ions measured in the ice-rises and S100 cores. PCA loadings were obtained at three different time intervals in the S100 core: 1737–2000, 1737–1949, and 1950–2000. Sources related to the different components are displayed in the bottom row.

Core	KC			KM		BI		S100					
	Annual			Annual		Annual		annual (1737–2000)		annual (1737–1949)		annual (1950–2000)	
Resolution	PC1	PC2	PC3	PC1	PC2	PC1	PC2	PC1	PC2	PC1	PC2	PC1	PC2
Loadings	0.17	0.52	-0.19	-0.20	0.64	0.03	0.65	0.16	0.54	0.23	0.44	0.03	0.73
MSA	0.46	-0.17	-0.19	0.40	0.03	0.43	-0.07	0.42	-0.07	0.43	-0.11	0.42	-0.08
Cl ⁻	0.13	0.59	0.35	-0.26	0.56	-0.03	0.56	-0.06	0.79	-0.08	0.74	0.14	0.60
NO ₃ ⁻	0.33	0.47	0.08	0.30	0.50	0.30	0.48	0.37	0.23	0.30	0.45	0.38	0.23
SO ₄ ²⁻	0.44	-0.11	-0.22	0.40	0.07	0.43	-0.06	0.42	-0.09	0.43	-0.13	0.42	-0.10
Na ⁺	0.46	-0.19	-0.11	0.40	0.03	0.40	-0.10	0.41	-0.06	0.41	-0.10	0.42	-0.05
K ⁺	0.45	-0.15	0.11	0.39	0.08	0.43	-0.08	0.41	-0.10	0.41	-0.11	0.40	-0.17
Mg ²⁺	0.17	-0.24	0.85	0.40	0.10	0.43	-0.03	0.39	0.02	0.36	0.05	0.39	-0.07
Ca ²⁺	51	22	12	76	18	65	24	70	15	60	17	69	16
Explained Variance (%)	sea-salts	biogenic mixed	terrestrial	sea-salts terrestrial	biogenic mixed	sea-salts terrestrial	biogenic mixed	sea-salts terrestrial	biogenic mixed	sea-salts terrestrial	biogenic mixed	sea-salts terrestrial	biogenic mixed
Source	sea-salts	biogenic mixed	terrestrial	sea-salts terrestrial	biogenic mixed	sea-salts terrestrial	biogenic mixed	sea-salts terrestrial	biogenic mixed	sea-salts terrestrial	biogenic mixed	sea-salts terrestrial	biogenic mixed

Table 4. Median Cl^-/Na^+ ratio (expressed in $\mu\text{mol L}^{-1}$), ssNa^+ , and nssNa^+ , and percentage of mean nssNa^+ to mean total Na^+ in the KC, KM, BI, and S100 cores. Since some of the calculated ssNa^+ values in the KC core were negative, ssNa^+ statistics are shown considering all data points, and only positive ssNa^+ values (sample rejection percentage is shown in parenthesis).

Site	Period (years)	Cl^-/Na^+	ssNa^+ ($\mu\text{mol L}^{-1}$)		nssNa^+ (crustal) ($\mu\text{mol L}^{-1}$)	Mean nssNa^+ to mean total Na^+ (%)
			All values	Only positive values		
KC	1958–2007	1.2	8.3	8.7 (5 %)	0.4	19
KM	1995–2012	1.3	56.6	56.6 (0%)	0.5	0.6
BI	1996–2012	1.2	18.6	18.6 (0 %)	0.3	1.4
S100	1737–2000	1.0	20.1	20.1 (0 %)	0.2	0.5
S100	1995–2000	1.0	143.7	143.7 (0 %)	-0.1	0.0
S100	1737–1949	1.0	14.7	14.7 (0 %)	0.3	2.1
S100	1950–2000	1.0	96.3	96.3 (0 %)	0.0	0.2

Table 5. Median of ss- and nss-fractions in the KC, KM, BI, and S100 cores. Percentage of negative nss-values for each ion is shown in parenthesis. Negative ss-values in the KC core are due to the 5 % of ssNa⁺ negative values obtained in section 3.4.

Core	Period (years)	Cl ⁻		SO ₄ ²⁻			K ⁺	Mg ²⁺		Ca ²⁺	
		ss	nss	ss	nss	ss	nss	ss	nss	ss	nss
KC	1958–2007	9.7	0.6 (32 %)	0.5	1.2 (4 %)	0.2	0.0 (27 %)	0.9	0.0 (43 %)	0.2	0.3 (5%)
KM	1995–2012	65.6	4.7 (12 %)	3.4	0.7 (39 %)	1.1	0.2 (13 %)	6.2	0.1 (48 %)	1.1	0.4 (0 %)
BI	1996–2012	21.6	1.0 (11 %)	1.1	0.8 (26 %)	0.4	0.1 (4 %)	2.0	0.0 (51 %)	0.4	0.2 (0 %)
S100	1737–2000	23.3	-2.8 (85 %)	1.2	-0.1 (53 %)	0.4	0.0 (45 %)	2.2	-0.3 (76 %)	0.4	0.1 (0 %)
S100	1995–2000	166.7	-29.3 (91 %)	8.6	-4.9 (80 %)	2.9	0.0 (50 %)	15.8	-5.5 (74 %)	2.9	-0.1 (56 %)
S100	1737–1949	17.0	-1.5 (80 %)	0.9	0.1 (36 %)	0.3	0.0 (45 %)	1.6	-0.2 (76 %)	0.3	0.2 (8 %)
S100	1950–2000	111.7	-18.6 (93 %)	5.8	-2.8 (83 %)	1.9	0.0 (43 %)	10.6	-2.6 (76 %)	1.9	0.0 (47 %)

Table 6. Median of MSA/nssSO₄²⁻ ratios, and bio-nssSO₄²⁻ in the KC, KM, BI, and S100 cores. Statistics for the MSA/nssSO₄²⁻ ratio are presented considering all values, and only positive values (sample rejection percentage is shown in parenthesis). In addition, the percentage of mean bio-nssSO₄²⁻ to mean total SO₄²⁻ is shown for all the cores.

Site	Period (years)	MSA/nssSO ₄ ²⁻		bio-nssSO ₄ ²⁻ (μmol L ⁻¹)	Mean bio-nssSO ₄ ²⁻ to mean total SO ₄ ²⁻ (%)
		All values	Only positive values		
KC	1958–2007	0.1	0.1 (4 %)	1.0	58
KM	1995–2012	0.1	0.3 (39 %)	1.9	46
BI	1996–2012	0.3	0.3 (26 %)	2.1	107
S100	1737–2000	0.0	0.3 (53 %)	0.7	37
S100	1995–2000	0.0	0.2 (80 %)	0.5	17
S100	1737–1949	0.2	1.0 (36 %)	0.7	72
S100	1950–2000	0.0	0.2 (83 %)	0.7	24

Table 7. Median annual nssSO₄²⁻ concentrations (in μmol L⁻¹) in the KC, KM, BI, and S100 firn/ice cores. (-) Not re-calculated.

Site	Period (years)	nssSO ₄ ²⁻ (μmol L ⁻¹)		
		$k_{\text{seawater}}=0.06$	$k'=0.02$	$k'=0.03$
KC	1958–2007	1.4	-	-
KM	1995–2012	0.8	-	-
BI	1996–2012	1.3	-	-
S100	1737–2000	0.3	0.9	0.7
S100	1995–2000	-2.3	2.3	1.2
S100	1737–1949	0.3	0.8	0.7
S100	1950–2000	-1.7	1.2	0.6

Figures

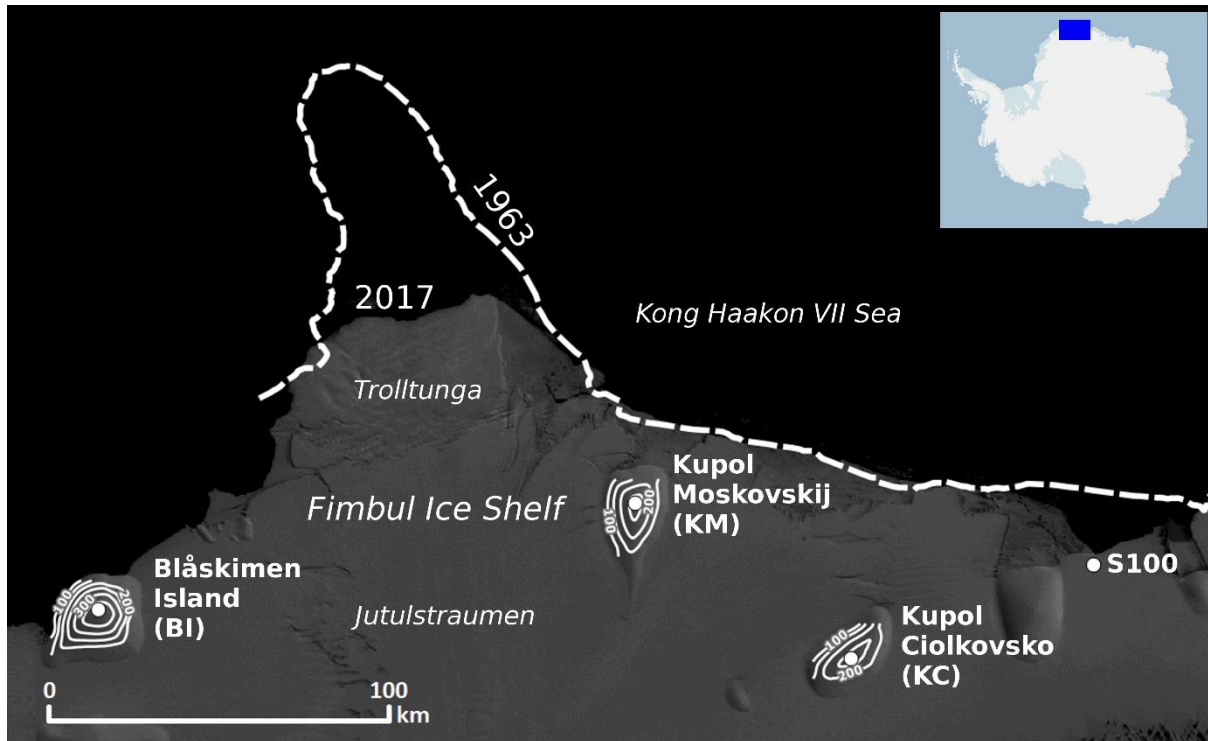


Figure 1. Satellite image of Fimbul Ice Shelf (FIS) showing the KC, KM, BI, and S100 core sites, Jutulstraumen, and Trolltunga. In addition, 50-m contours are shown at each ice-rise, as derived from GPS profiles (V. Goel, personal communication, 2016). In addition, the dashed line shows the extent of Trolltunga according to Corona Satellite data from 1963 (J. van Oostveen, personal communication, 2017). Map image is from the MODIS Mosaic of Antarctica (MOA). Additional information regarding the sampling sites and traverses in FIS can be found in Schlosser et al. (2014) and Vega et al. (2016).

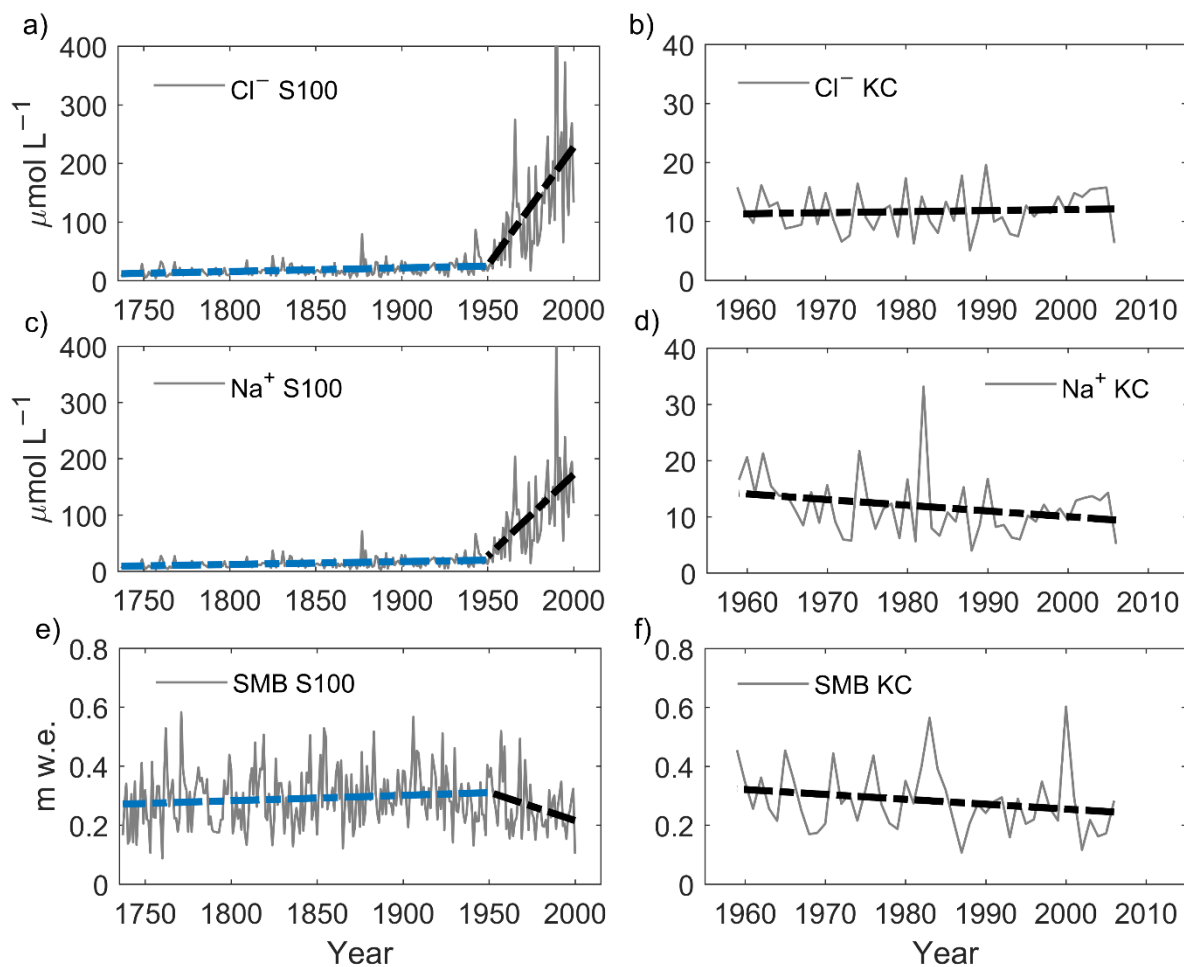


Figure 2. Annual sea-salt (Cl^- and Na^+) concentrations and surface mass balance (SMB) in the two longest records retrieved at Fimbul Ice shelf, S100, (a), (c), and (e), and KC, (b), (d) and (f). Linear trends in Cl^- and Na^+ concentrations, and SMB measured in the S100 core are shown for two different periods: 1737–1949 (blue dashed line) and 1950–2000 (black dashed line) in (a), (c), and (e), respectively. Linear trends in Cl^- and Na^+ concentrations, and SMB measured in the KC core are shown for the period 1958–2007 (black dashed line) in (b), (d) and (f), respectively. Significance, slope, and standard error of the linear regressions are given in Table S3.

5

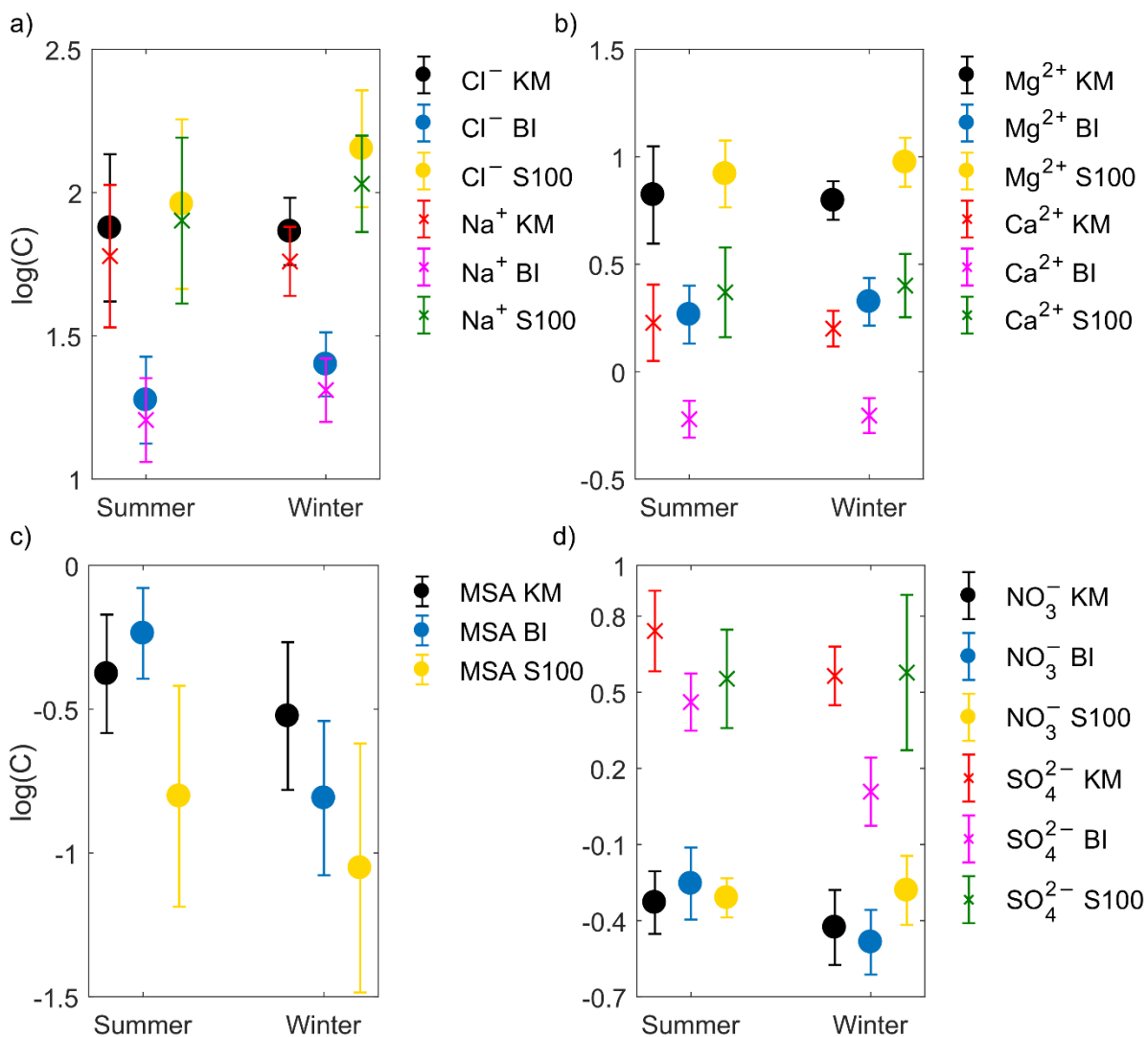


Figure 3. Sub-annual variability of selected ions, Cl⁻ and Na⁺ (a), Mg²⁺ and Ca²⁺ (b), MSA (c) and NO₃⁻ and SO₄²⁻ (d) in cores KM, BI, and S100. Mean summer and winter concentrations were calculated for the months NDJFMA, and MJJASO, for a period of 16, 15, and 5 years in the KM, BI, and S100 cores, respectively.

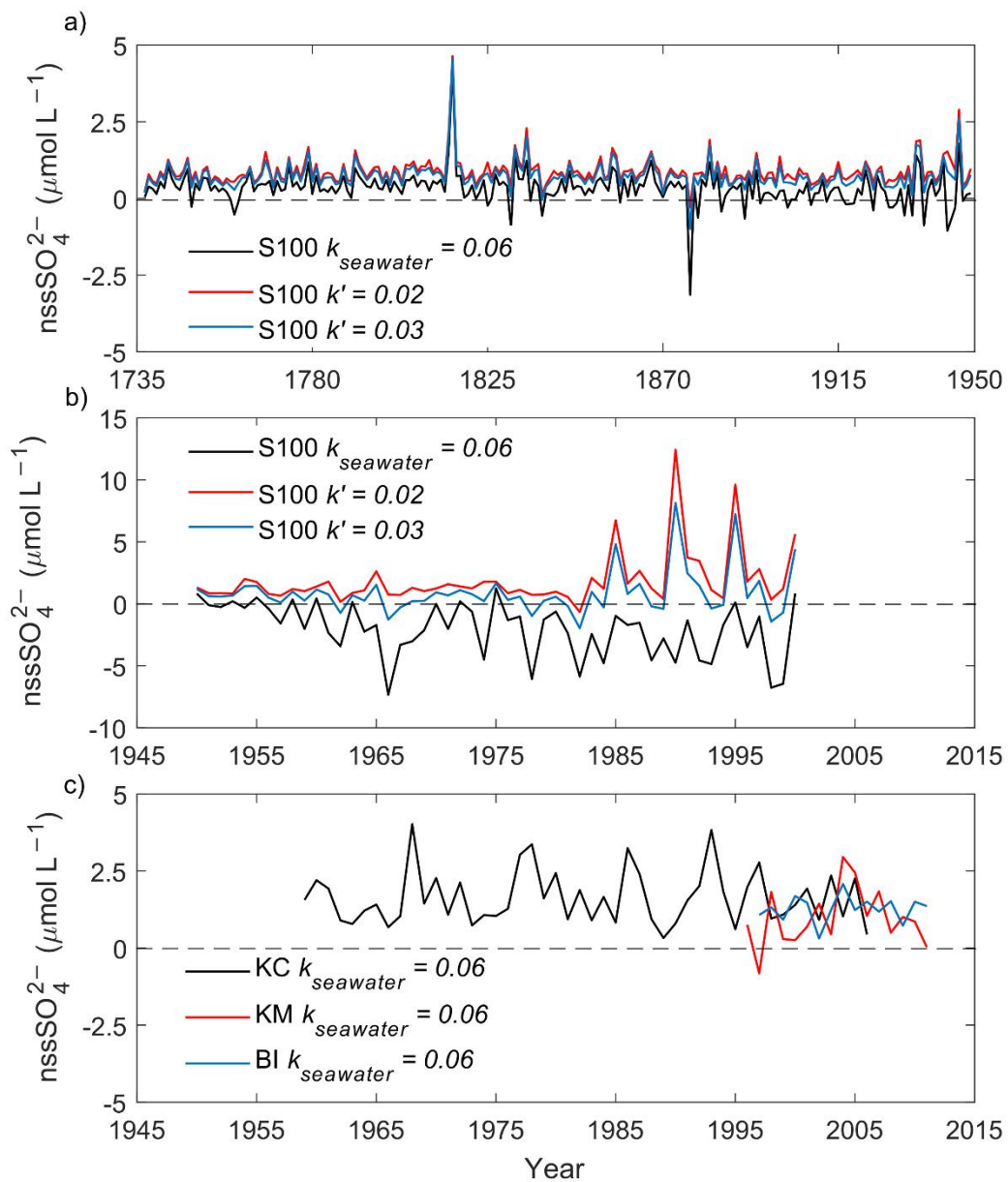


Figure 4. Annual nssSO_4^{2-} concentrations in the S100 core between a) 1737–1949, b) 1950–2000, and c) in the KC, KM, and BI cores. nssSO_4^{2-} recalculated using $k_{\text{seawater}}=0.06$, $k'=0.02$ and $k'=0.03$ are shown in panels a) and b) with black, red and blue lines, respectively. nssSO_4^{2-} in the KC, KM, and BI cores was calculated using $k=0.06$.

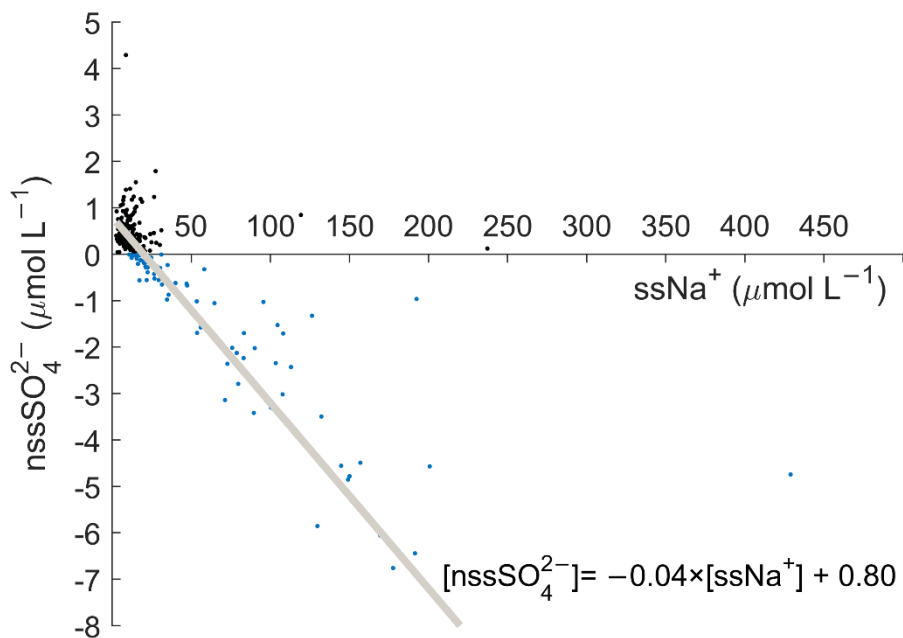


Figure 5. Scatter plot of annual nssSO_4^{2-} vs. ssNa^+ concentrations in the S100 core. nssSO_4^{2-} was calculated using the seawater ratio as described in section 2.3 and using a $k_{\text{seawater}}=0.06$ (in $\mu\text{mol L}^{-1}$). Positive nssSO_4^{2-} values are denoted with black dots, while negative values are denoted with blue dots. A linear regression was calculated using all nssSO_4^{2-} data points to infer corrected k value (k'), following the approach by Wagenbach et al. (1998).

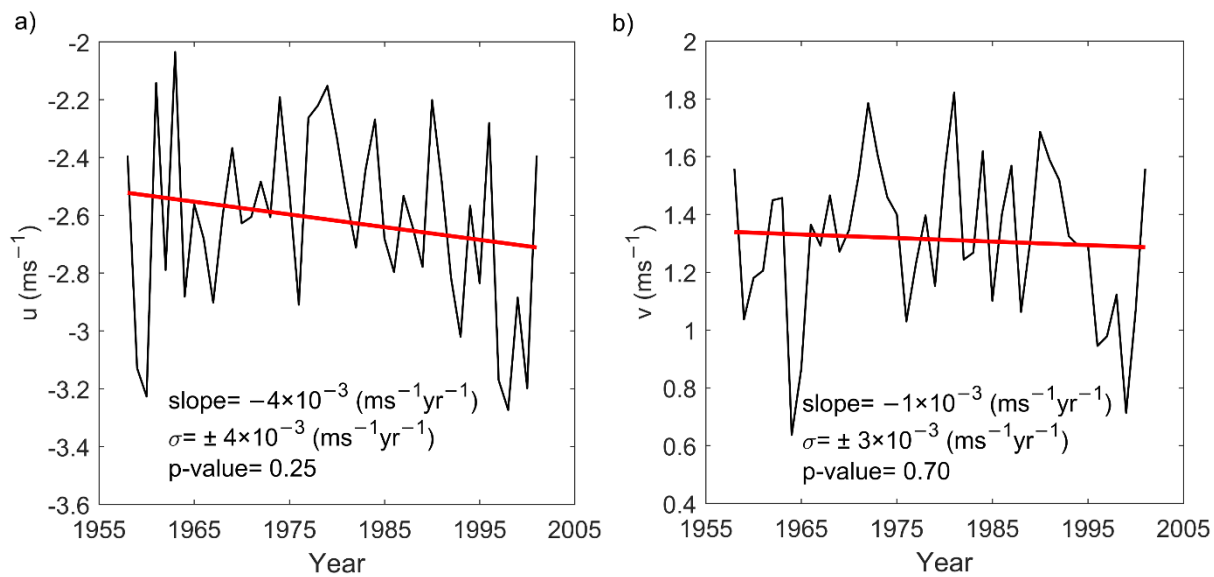


Figure 6. Annual averages of monthly a) zonal, and b) meridional wind speeds (ERA40) for the area (69°S–71°S, 3.5°W–5°E) between 1958–2001. Slope, standard deviation, and p -value of the linear regression are shown in the figure.